WEIGHTED LIKELIHOOD FUNCTION OF MULTIPLE STATISTICAL PARAMETERS TO RETRIEVE 2D TRUS-MR SLICE CORRESPONDENCE FOR PROSTATE BIOPSY

J. Mitra[*†], *S. Ghose*[*†], *D. Sidibé*[*], *A. Oliver*[†], *R. Martí*[†], *X. Lladó*[†], *J. C. Vilanova*[◇], *J. Comet*[‡], *F. Meriaudeau*[*]*

[*] Université de Bourgogne, Le2i UMR-CNRS 6306, Le Creusot, France
[†] Universitat de Girona, Computer Vision and Robotics Group, Girona, Spain
[◇] Girona Magnetic Resonance Center, Girona, Spain
[‡] Hospital Dr. Josep Trueta, Girona, Girona, Spain.

(jhimli.mitra/soumya.ghose/dro-desire.sidibe/fabrice.meriaudeau)@u-bourgogne.fr, (aoliver/marly/llado)eia.udg.edu

ABSTRACT

This paper presents a novel method to identify the 2D axial Magnetic Resonance (MR) slice from a pre-acquired MR prostate volume that closely corresponds to the 2D axial Transrectal Ultrasound (TRUS) slice obtained during prostate biopsy. The shape-context representations of the segmented prostate contours in both the imaging modalities are used to establish point correspondences using Bhattacharyya distance. Thereafter, Chi-square distance is used to find the prostate shape similarities between the MR slices and the TRUS slice. Normalized mutual information and correlation coefficient between the TRUS and MR slices are computed to find the information theoretic similarities between the TRUS-MR slices. The maximum of the weighted likelihood function of the afore-mentioned statistical similarity measures finally yields the MR slice that closely resembles the TRUS slice acquired during the biopsy procedure. The method is evaluated for 20 patient datasets and close matches with the ground truth are obtained for 16 cases.

Index Terms— Prostate biopsy, 2D TRUS/3D MR correspondence, shape similarity, image similarity, weighted likelihood function.

1. INTRODUCTION

Prostate cancer has been a major cause of mortality among human males in the European and American societies since the last 25 years. Therefore, prostate cancer screening programs are conducted where a patient with abnormal findings after a digital rectal examination, serum Prostate Specific Antigen (PSA) level over 4.0 ng/ml and PSA velocity between $0.4 - 0.75$ ng/ml/yr is generally advised for a prostate biopsy for histopathological examination of the prostate tissues. The appearance of malignant lesions in a Transrectal

Ultrasound (TRUS) guided needle biopsy is mostly hypoechoic and the accuracy of finding such lesions is typically 43% in sonography [1]. Approximately $25\% - 42\%$ of cancer lesions can also be isoechoic under TRUS. Therefore, the chance to diagnose hypoechoic lesions from TRUS guided biopsy that are malignant is $\leq 57\%$ [2]. Vilanova et al. [3] demonstrated that the accuracy of Magnetic Resonance Imaging (MRI) to diagnose prostate cancer is $72\% - 76\%$. Therefore, for men deemed to be at risk of prostate cancer, fusion of pre-biopsy MR images onto interventional TRUS images might increase the overall biopsy accuracy [4].

Fusion of pre-biopsy MR on interventional TRUS may be done in several ways. An Electro Magnetic (EM) tracker attached to the 2D TRUS probe may be used that sweeps the prostate to reconstruct a 3D TRUS volume. The 3D TRUS volume is then fused with the MR volume to obtain the spatial position of the 2D TRUS slice during biopsy within the pre-biopsy MR volume [4]. On the other hand, a 3D TRUS probe may be directly used to acquire 3D TRUS volume and a volume-volume registration may be performed [5, 6]. However, neither 3D TRUS probe is commonly available in diagnostic centers nor the use of the EM tracker is an established clinical practice. Therefore, intending to solve the 2D TRUS-MR slice correspondence problem, we propose a method based on Chi-square distance of shape-context representations of the prostate contours and information theoretic measures like Normalized Mutual Information (NMI) and Correlation Coefficient (CC) of the TRUS-MR slices. Finally, the maximum of the Weighted Likelihood (WL) function of the Chi-square distance and the NMI and CC parameters is computed to find the MR slice that closely matches the TRUS slice. The novelties of the proposed work may be summarized as follows:
1) Using shape context representations of the contours to find prostate shape similarities between TRUS and MR slices.
2) Combining shape information with intensity information through a WL framework to identify the correct MR slice.

In the remaining paper, section 2 describes the proposed

(a)   (b)
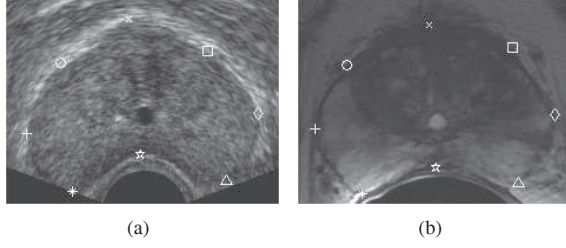
Fig. 1. Point correspondences example. (a) contour points in TRUS, (b) point correspondences of (a) in MR.

method in detail, section 3 provides the results and discussions followed by the conclusions in section 4.

2. THE PROPOSED METHOD

In this work, the prostate is manually segmented from the 2D TRUS axial slice and the pre-biopsy axial MR volume where the TRUS slices are considered to be parallel to the MR axial plane. However, we will finally use the fast automatic prostate segmentation methods in both MR and US modalities by Ghose et al. [7, 8]. The shape similarity measure of Chi-square distance on shape-context representations of point correspondences is explained in section 2.1, the information theoretic image similarity measures like NMI and CC are explained in section 2.2 with explanation of WL approach in section 2.3.

2.1. Shape Similarities

The segmented prostate contour points are uniformly sampled using fixed Euclidean distance of ε i.e. if c_i is a contour point, $i = 1, \ldots, N$, then maximize the following equation

$$\arg\max_j \|c_i - c_j\|^2 \leq \varepsilon, \quad i \neq j. \tag{1}$$

The number of uniformly sampled points given as n, each sample point c_i may be represented by a shape descriptor that is a $n-1$ length vector of log-polar relative distances to points c_j, where $i \neq j$. The shape descriptor is binned into a histogram that is uniform in log-polar space and this histogram is the shape-context representation of a contour point [9] i.e. c_i is represented by a histogram $h_i(k, \theta)$ such that

$$h_i(k, \theta) = \#\{c_j, i \neq j \quad : \quad (c_i - c_j) \in bin(k, \theta)\}. \tag{2}$$

k is the $\log r = \log(\sqrt{(x_{i1} - x_{j1})^2 + (x_{i2} - x_{j2})^2})$ and $\theta = \tan^{-1}\frac{x_{j2} - x_{i2}}{x_{j1} - x_{i1}}$ of the relative distance $(c_i - c_j)$, where, $c_i = (x_{i1}, x_{i2})$ and $c_j = (x_{j1}, x_{j2})$. As suggested by Belongie et al. [9], a total of 5 bins are considered for k and 12 bins for θ that ensures that the histogram is uniform in log-polar space. This also means that more emphasis is given to the nearby sample points than those that are far away.

In the original work of Belongie et al. [9], the point correspondence between two shapes is obtained by a bipartite graph matching method. However, in this work we choose the Bhattacharyya distance [10] between the shape-context his-

tograms of two shapes to find the best point correspondence since it is fast to compute and statistically a robust measure to find correspondences in similar shapes like prostate contours in TRUS and MRI. Thus, to match a point c_i in a shape to a point c'_j in another shape, the Bhattacharyya coefficients between the shape-context histogram of c_i and all c'_j are computed and the c'_j that maximizes the relation in Eq. (3) is chosen as the corresponding point.

$$\arg\max_{c'_j} \sum_{k=1}^{5} \sum_{\theta=1}^{12} \sqrt{\hat{h}_i(k, \theta).\hat{h}'_j(k, \theta)}, \tag{3}$$

where, $\hat{h}_i(k, \theta)$ and $\hat{h}'_j(k, \theta)$ are the normalized shape-context histograms of c_i and c'_j respectively. Fig. 1 shows the contour correspondences overlaid on the TRUS and MR prostate shapes.

After the corresponding points are identified, the Chi-square (χ^2) distances between the TRUS slice and each of the MR slices are calculated based on the corresponding shape-context histograms and is given by $\mathcal{C}_{ij}$ in Eq. (4). The final distance is the sum of all the χ^2 distances of the corresponding points (shape-context histograms) in TRUS and MR and is given by $\mathcal{H}$ in the following equation.

$$\mathcal{C}_{ij} = \frac{1}{2} \sum_{k=1}^{5} \sum_{\theta=1}^{12} \frac{(\hat{h}_i(k, \theta) - \hat{h}'_j(k, \theta))^2}{\hat{h}_i(k, \theta) + \hat{h}'_j(k, \theta)}, \quad \mathcal{H} = \sum_{i=1}^{l} \mathcal{C}_{ij}, \tag{4}$$

where, l is the number of point correspondences. The TRUS-MR slice pair with minimum sum of χ^2 distance ($\mathcal{H}$) is identified and its significance will be discussed in the following subsection.

2.2. Image Similarities

Image similarity measures have been extensively used in multimodal image registration problem to ensure that the moving image is transformed with close resemblance to the fixed image. In this work, our problem is to find an MR slice in the volume that closely resembles the TRUS slice. Therefore, to find such similarity we employ the well-known NMI and CC as image similarity measures. It may be noted here that in an image registration problem, either NMI or CC is used as a similarity measure. However, as demonstrated by Fei et al. [11] that better registration accuracies are obtained with CC in low resolution and with MI in high resolution and lower registration accuracies are obtained when CC is used in high resolution and MI in low resolution respectively. Related to our problem, some TRUS slices have smaller prostate sizes than the other. Therefore, considering the variability in prostate sizes we decided to use both NMI and CC as similarity measures.

The TRUS-MR slice pair identified with the minimum $\mathcal{H}$ as obtained from Eq. (4) is used to retrieve the 2D rigid transformation (inplane rotation and translation) parameters between them; and the remaining MR slices in the volume are rigidly registered with the TRUS slice using the same parameters. This registration step ensures similar 2D inplane rigid alignment of all the MR slices of the volume with the

Table 1. Ground truth (GT) and results for MR slices corresponding to a TRUS slice. The matched cases are shown in italics.

Patients/MR Slice	1	2	3	4	5	6	7	8	9	10	11	12	13	14	15	16	17	18	19	20	Agreement (%)
GT (Expert 1)	6	8	9	7	6	10	6	10	5	7	6	5	12	8	6	5	7	7	6	7	**45%**
GT (Expert 2)	2	7	6	5	6	9	6	8	7	6	6	4	*13*	8	*4*	8	*10*	9	6	7	**75%**
Our method	3	7	3	6	5	9	6	8	8	6	9	3	*13*	3	*4*	8	*10*	6	7	5	-

2D TRUS slice.

After the alignment of the MR volume with the TRUS slice, pairwise NMI and CC are computed for each MR-TRUS slice pair. The NMI is an information theoretic measure that tries to reduce the joint entropy of the images [12] and is given by

$$\text{NMI} = \frac{H(M) + H(T)}{H(M,T)} \qquad (5)$$

where, $H(M)$ and $H(T)$ are the marginal entropies of the MR (M) and TRUS (T) images respectively, and $H(M,T)$ is the joint entropy of the images. $H(M,T)$ can be written using probability theory as

$$H(M,T) = -\sum_{M,T} p(M,T) \log \left[p(M,T) \right], \qquad (6)$$

where, $p(M,T)$ is the joint probability distribution of the images obtained from their joint histogram.

The CC gives a linear dependence between two random variables $M(m)$ and $T(t)$ [13] as intensities of the MR and the TRUS images respectively, and is defined as:

$$CC(M,T) = \frac{\sum \left(T(t) - \overline{T}(t) \right) \left(M(m) - \overline{M}(m) \right)}{\sqrt{\sum \left(T(t) - \overline{T}(t) \right)^2 \sum \left(M(m) - \overline{M}(m) \right)^2}}. \qquad (7)$$

m and t are the pixel positions in the TRUS and MR images respectively. $\overline{M}(m)$ and $\overline{T}(t)$ are the average pixel intensities for the overlapping regions.

2.3. Weighted Likelihood (WL)

The MR slice corresponding to the observed TRUS slice should ideally be the one with lowest $\mathcal{H}$ obtained from section 2.1 and maximized NMI and CC as obtained from section 2.2. The values of these statistical shape and image similarity measures are consecutively transformed into pdfs to accommodate our problem into the WL framework.

Given a set of random data $\mathbf{X} = \{\mathbf{x}_1 \ldots \mathbf{x}_n\}$ each having a pdf $p_i(\mathbf{x}_i;\ \xi)$, $i = 1 \ldots n$ and ξ the parameter, the WL function of the pdfs [14] is given by

$$WL(\mathbf{X}; \xi) = \prod_{i=1}^{n} p_i(\mathbf{x}_i;\ \xi)^{\lambda_i}, \qquad (8)$$

where, λ_i are the weights that may be determined depending on the application. In this work, the set of random variables is $\mathbf{X} = \{\mathcal{H}', \text{NMI}, \text{CC}\}$, where $\mathcal{H}' = 1 - \mathcal{H}$ and their respective probability values constituting the pdfs in Eq. (8). The ξ being each MR slice of a volume, a separate WL value is generated for each TRUS-MR slice pair. Finally, the MR slice that provides the maximum WL function value is chosen as the slice that closely corresponds to the TRUS slice.

3. RESULTS AND DISCUSSIONS

The results are validated against the ground truth obtained from an expert radiologist and an expert urologist for 20 patients axial mid-gland TRUS slices. The axial MR slices have slice thickness of 3pixels with inter-slice gap of 3.5 pixels where the pixel dimension is 0.2734×0.2734 mm. The weight for $\lambda_{\mathcal{H}}$ of section 2.3 is computed from a training phase and is obtained as the average probability of obtaining the MR slice equal or $[-1, +1]$ slice away from either or both the expert ground truth that employs only $\mathcal{H}'$ for 20 patients in a leave-one-patient-out framework. Similarly, λ_{NMI} and λ_{CC} are also computed yielding probabilistic weights of $\lambda = 0.35, 0.45, 0.25$ for $\mathcal{H}'$, NMI and CC respectively. Table 1 shows the ground truth of the axial MR slice corresponding to an axial TRUS slice provided by the experts (independently) and the results we obtained using our method.

It is observed from Table 1 that the automatic MR slice choice matched at least one of the expert ground truth for 9 out of 20 cases wherein the experts differ in their opinions for 5 patient cases $(2, 6, 10, 12 \& 13)$ with $[-1, +1]$ slice difference and for 9 patient cases $(1, 3, 4, 8, 9, 15, 16, 17 \& 18)$ with $2 - 4$ slice differences. The expert choices matched exactly in 6 cases $(5, 7, 11, 14, 19 \& 20)$ out of which our result matched exactly for one patient case 7 and $[-1, +1]$ slice away for patients 5 & 19 respectively. For all 14 cases, where the experts disagreed on their opinions, our results either matched exactly or are $1 - 2$ slices above/below at least one expert or are between the expert choices for 13 cases except patient 3. Since, the expert choices agreed exactly and $[-1, +1]$ slice away in 11 out of 20 cases, the experts are in agreement by 55%.

Comparing each of the expert ground truth independently with our method, the exact match with expert 1 ground truth is only for patient 7 while $[-1, +1]$ (a statistically significant 20% error) slice away for 8 patients $(2, 4, 5, 6, 10, 13, 18 \& 19)$. Therefore, 9 out of 20 cases i.e. 45% results are in agreement with that of the ground truth of expert 1. Similarly for 9 cases $(2, 6, 7, 8, 10, 13, 15, 16 \& 17)$ our results exactly matched expert 2 ground truth and are 1 slice away for 6 patient cases $(1, 4, 5, 9, 12 \& 19)$. This signifies that the results of our method are in 75% agreement with that of expert 2 ground truth. The inter-expert variability in the choice of MR slice being high (55% agreement), our method performs better with an agreement of 75% for expert 2 (Table 1) that shows an increase in performance by 36.36%. However, the slice choice by our method are in 45% agree-
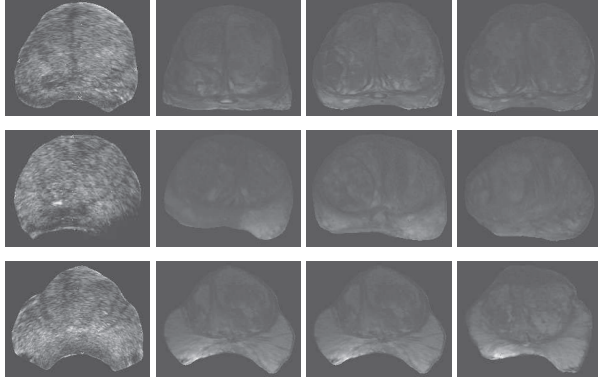
Fig. 2. TRUS-MR corresponding slices. Rows (top to bottom) show patient cases 9, 3 and 11 respectively. The 1st column shows the TRUS slices, the 2nd and the 3rd show the expert ground truth for the MR slices and the last column the obtained result using our method.

ment with expert 1 ground truth (Table 1) which indicates a decrease in performance by 18.18%.

The results obtained by our method for patients 3 and 11 do not match any of the expert ground truth and are neither $[-1, +1]$ slice away from either of the ground truth. The reason for the failure in these cases could be the use of deterministic weight values instead of adaptive weight values of λ i.e. instead of using fixed weights for $\mathcal{H}'$, NMI and CC for all patient cases, the weights may be altered depending on the values of $\mathcal{H}'$, NMI and CC obtained for each of the TRUS-MR pair on a probabilistic scale. Fig. 2 shows patient case 9 where the result obtained is one slice below than that of the ground truth of Expert 2 as shown in Table 1. Fig. 2 also shows patient cases 3 and 11 where the results are not close to any of the expert ground truth.

The method has been implemented in MATLAB and the complete process takes 3 secs on an average to find out the corresponding MR slice from a set of $12 - 14$ slices. It is to be noted that Xu et al. [4] employed an EM tracker to locate the spatial position of the 2D TRUS slice (during guided biopsy) in the 3D TRUS volume. Thereafter, to compensate for the prostate motion, the sum-of-squared difference (SSD) between the maximum translational and rotational TRUS slices within a short time frame (during TRUS guided biopsy) and the corresponding spatial 2D TRUS slices obtained in the 3D TRUS volume was minimized. However, in our case the exact orientation of the 2D TRUS probe relative to the prostate is unknown. Therefore, we may similarly propose the minimization of SSD or NMI between the 2D MR slice corresponding to the 2D TRUS slice (obtained from our method) and the corresponding MR slices of the maximum translational and rotational TRUS slices during biopsy. Hence, our proposed method provides a good starting point for multimodal registration and may be used as a substitute of EM tracker and 3D TRUS probe that are generally not used for biopsy.

4. CONCLUSIONS

A method to find out 2D MR slice correspondence of a 2D axial TRUS slice during biopsy has been reported in this paper. The method is based on statistical shape and image similarity measures, a weighted combination of which provides likelihood values for the MR slices. The method is fast in finding out MR correspondences that are nearly the same as the ground truth obtained from two experts. Since EM tracker is not easily available in hospitals in Europe and 3D TRUS is normally not employed for biopsy purposes, our proposed method may provide a good starting point for multimodal fusion of TRUS-MR images to improve the sampling of biopsy tissues. Although the results reported in this paper are validated only for mid-gland or close to mid-gland axial slices, the validations for the base and apex TRUS axial slices and TRUS sagittal slices and cross-validation of our method with the use of an EM tracker have been left as future works.

5. REFERENCES

[1] P. Carroll and K. Shinohara, "Transrectal ultrasound guided prostate biopsy," Tech. Rep., Dept. of Urology, Univ. of California, San Francisco, 2010, http://urology.ucsf.edu/patientGuides.html, accessed [30th Dec, 2010].

[2] H. A. Bogers et al., "Contrast-enhanced three-dimensional power Doppler angiography of the human prostate: correlation with biopsy outcome," *Urology*, vol. 54, no. 1.

[3] J. C. Vilanova et al., "Usefulness of prebiopsy multi-functional and morphologic MRI combined with the free-to-total PSA ratio in the detection of prostate cancer," *Am. Jour. of Roentgenology*, vol. 196, no. 6, pp. W715–W722, 2011.

[4] S. Xu et al., "Real-time MRI-TRUS fusion for guidance of targeted prostate biopsies," *Comp. Aid. Surg.*, vol. 13, no. 5, pp. 255–264, 2008.

[5] M. Baumann et al., "Prostate biopsy assistance system with gland deformation estimation for enhanced precision," in *Proc. of MICCAI*, September 2009, vol. LNCS 5761, pp. 57–64.

[6] M. Baumann et al., "Prostate biopsy tracking with deformation estimation," *Med. Imag. Anal., In Press*, 2011.

[7] S. Ghose et al., "Prostate segmentation with texture enhanced active appearance model," in *Proc. IEEE SITIS*, December 2010, pp. 18–22.

[8] S. Ghose et al., "A probabilistic framework for automatic prostate segmentation with a statistical model of shape and appearance," in *Proc. IEEE ICIP*, September 2011, pp. 725–728.

[9] S. Belongie et al., "Shape matching and object recognition using shape contexts," *IEEE Trans. on Patt. Anal. and Mach. Intell.*, vol. 24, no. 4, pp. 509–522, 2002.

[10] A. Bhattacharyya, "On a measure of divergence between two statistical populations defined by their probability distribution," *Bull. of the Calcutta Math. Soc.*, vol. 35, pp. 99–110, 1943.

[11] B. W. Fei et al., "Slice-to-volume registration and its potential application to interventional MRI-guided radio-frequency thermal ablation of prostate cancer," *IEEE Trans. on Med. Imag.*, vol. 22, no. 4, pp. 515–525, 2003.

[12] C. Studholme et al., "An overlap invariant entropy measure of 3D medical image alignment," *Patt. Recog.*, vol. 72, no. 1, pp. 71–86, 1999.

[13] W. H. Press et al., *Numerical recipes in C: The Art of Scientific Computing*, Cambridge Univ. Press, London, UK, 2nd edition, 1993.

[14] F. Hu and J. V. Zidek, "The weighted likelihood," *The Canadian Jour. of Stats.*, vol. 30, no. 3, pp. 347–371, 2002.